

Direct visualization of aging in colloidal glasses

Rachel E. Courtland and Eric R. Weeks †

Physics Department, Emory University, Atlanta, GA 30322 USA

Abstract. We use confocal microscopy to directly visualize the dynamics of aging colloidal glasses. We prepare a colloidal suspension at high density, a simple model system which shares many properties with other glasses, and initiate experiments by stirring the sample. We follow the motion of several thousand colloidal particles after the stirring and observe that their motion significantly slows as the sample ages. The aging is both spatially and temporally heterogeneous. Furthermore, while the characteristic relaxation time scale grows with the age of the sample, nontrivial particle motions continue to occur on all time scales.

PACS numbers: 64.70.Pf, 82.70.Dd, 61.43.Fs

Submitted to: *J. Phys.: Condens. Matter*

1. Introduction

Colloidal suspensions have long been used as model systems to study the glass transition [1, 2, 3, 4, 5]. As the concentration of a colloidal suspension is increased, the motion of the colloidal particles becomes increasingly slowed. The glass transition is considered to occur at the concentration at which particle motion ceases to be diffusive on long time scales [5]. Recent work has studied the behavior of simple colloidal suspensions as this transition is approached [6, 7, 8]. In this paper we examine the behavior of glassy samples. Unlike supercooled colloidal fluids, the behavior of a colloidal glass depends on the history of the sample: particle motion becomes increasingly slowed as the sample ages [9, 10, 11, 12, 13]. We use confocal microscopy to study the three-dimensional motions of colloidal particles in an aging colloidal glass. We find that aging occurs due to slight rearrangements which are both spatially and temporally heterogeneous. Moreover, even after the sample has aged for long times, small but significant motions occur on short time scales. Previous work has seen similar evidence of spatial and temporal heterogeneities in aging systems [9, 16, 17, 18].

† To whom correspondence should be addressed (weeks@physics.emory.edu)

2. Experimental Methods

We use poly-(methylmethacrylate) (PMMA) particles of radius $a = 1.18 \mu\text{m}$ and polydispersity $\sim 5\%$, sterically stabilized by a thin layer of poly-12-hydroxystearic acid. The particles are dyed with rhodamine and suspended in a mixture of organic solvents (cyclohexylbromide and decalin) that closely matches both the density and index of refraction of the particles. We use a scanning laser confocal microscope to acquire images of a viewing volume of $63 \mu\text{m} \times 58 \mu\text{m} \times 12 \mu\text{m}$ at the rate of 3 images per minute. The viewing volume typically contains ~ 2400 particles. We focus at least $60 \mu\text{m}$ away from the cover slip of the sample chamber to avoid wall effects. We identify particles with a horizontal accuracy of $0.03 \mu\text{m}$ and a vertical accuracy of $0.05 \mu\text{m}$ and track them in three dimensions over the course of the experiment [14, 15].

The control parameter for the colloidal phase behavior is the sample volume fraction ϕ . While the rhodamine imparts a slight charge upon the particles, their phase behavior, $\phi_{freeze} = 0.38$ and $\phi_{melt} = 0.42$, is similar to that of hard spheres ($\phi_{freeze} = 0.494$ and $\phi_{melt} = 0.545$). We observe a glass transition at $\phi_g \approx 0.58$, in agreement with what is seen for hard spheres [1, 8]. We examined samples with volume fractions ranging $\phi \approx 0.58$ to $\phi \approx 0.62$. These samples form small crystals which nucleate at the coverslip, but do not form crystals within the bulk of the sample even after several weeks.

In order to initialize the system, a small length of wire is inserted into each sample chamber. After placing a sample on the microscope stage, a handheld magnet is used to pull and rotate the wire through the sample for several minutes. The subsequent particle dynamics are reproducible after this stirring. Within a minute of ending the stirring, transient flows within the sample greatly diminish, and the particles move slowly enough to be identified and tracked. This defined our initial time $t = 0$ for each sample, although the results below are not sensitive to variations of this choice. During the course of the experiments, no crystallization was observed within the viewing volume. Note that in many aging studies, the initial sample is prepared by a temperature quench (which would correspond to a rapid increase of the volume fraction in our experiments). The initial conditions in our experiments correspond to a shear-melted sample; the volume fraction remains constant.

3. Results

As a glass ages, we expect dynamical properties to change with time. To investigate this, we consider small temporal portions of a data set and calculate the mean square displacement $\langle \Delta r^2 \rangle$ (MSD) for each portion, where the angle brackets indicate an average over all particles and all initial times within each temporal portion. Figure 1 displays the progression of the MSD curves of a colloidal glass ($\phi = 0.62$) over a period of two hours, showing a marked change as the sample ages. The data is divided logarithmically into segments according to the sample age t_w , the time waited since stirring, such that $t_w^{n+1} = c t_w^n$, where $c = 1.4$, $t_w^0 = 3.0$ minutes and $n = [1, 2, \dots, 11]$.

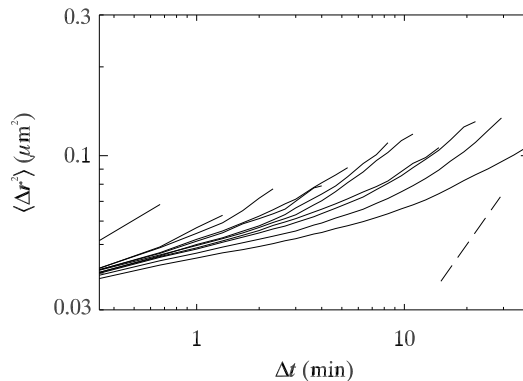


Figure 1. Mean square displacement versus lag time for a colloidal glass ($\phi \approx 0.62$). The total length of the data set is 120 min. Data is divided logarithmically according to sample age. The geometric mean ages of the curves, from left to right, are $\bar{t}_w = 3.0, 4.2, 5.9, 8.2, 12, 16, 23, 32, 44, 62, 87$ min. The dashed line has a slope of 1.

The MSD for a given t_w is calculated using data within the interval $[c^{-1}t_w, ct_w]$. The MSD behavior at low and intermediate lag times is consistent with that of super-cooled liquids [6, 7]. For $\Delta t < 30$ s (not shown), the MSD grows roughly linearly with Δt , corresponding to the diffusion of particles inside “cages” formed by neighboring particles [5, 6]. The MSD at intermediate lag times exhibits a plateau, as particles are locally confined by their neighbors. At larger lag times, the MSD curves each show a slight upturn, reminiscent of super-cooled liquids [13]. For super-cooled liquids, this upturn corresponds to cage rearrangements: the configuration of particles around a caged particle changes noticeably [6]. In our aging samples, we see similar, though smaller, motions, and the upturn in the MSD is less obvious than is seen in liquids. These motions, which change the local positions of particles, are likely related to cage rearrangements [12, 13]. Presumably these local rearrangements lead to the aging of the sample. However, unlike super-cooled liquids, the time scale for the upturn in the MSD depends strongly on the age of the sample, t_w , as is clear from Fig. 1 [13]. For larger values of t_w , the plateau extends over a larger range of Δt . This behavior has been seen before in a variety of aging systems [10, 11].

We observe also that the MSD of a colloidal glass does not evolve uniformly. Consider the four rightmost curves in Fig. 1, corresponding to $\bar{t}_w = 32, 44, 62,$ and 87 min. The first two curves ($\bar{t}_w=32, 44$ min) are virtually indistinguishable, showing that the dynamics have not changed within the imaging volume. However, the next two curves ($\bar{t}_w=62, 87$ min) are quite different, showing that the particles within the imaging volume have aged. This suggests that aging is in part temporally heterogeneous in our small observation volume. It is to be expected that if a larger volume was examined, such as in light scattering experiments, the dynamics would appear to evolve more smoothly with t_w [10, 11].

The temporal averaging used in calculating the MSD obscures some of the details of this temporal heterogeneity. However, it is unclear how to best study the dynamics

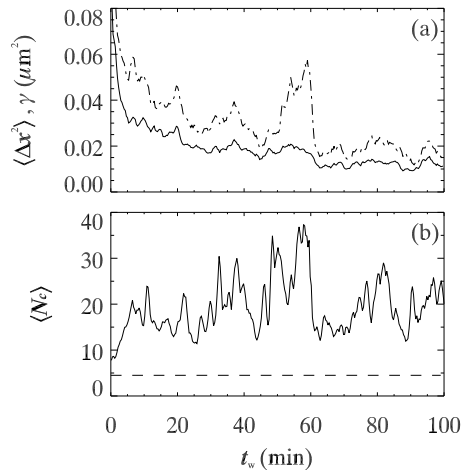


Figure 2. Various ensemble features as a function of sample age, t_w . The time lag is fixed ($\Delta T = 10$ min) and the data are the same as shown in Fig. 1. (a) $\langle \Delta x^2 \rangle$ and $\gamma = \sqrt{\langle \Delta x^4 \rangle / 3}$ (dashed). (The x component is used as the z component is noisier due to optical effects.) (b) Average number of particles in a cluster of mobile particles; see text for details. The dashed line indicates the average cluster size if mobile particles were randomly distributed.

given that the time scales for such dynamics may vary dramatically with the sample age t_w . Furthermore, the mobile particles responsible for the upturn in the MSD are only moving slightly farther than the immobile particles; the latter still move locally due to their Brownian motion. To help distinguish the rearranging particles from those which only move within their cage, we average the trajectory of each particle over 1 min. The results that follow are not sensitive to the choice of this averaging time.

To investigate the nature of the temporally heterogeneous aging, we choose a fixed lag time ΔT and study how the dynamical behavior changes with t_w . We might expect that for $t_w \ll \Delta T$, $t_w \approx \Delta T$, and $t_w \gg \Delta T$, we should see strikingly different behavior. We choose $\Delta T = 10$ min to allow us to resolve these three regimes with our data. The solid line in Figure 2(a) shows $\langle \Delta x^2 \rangle_{\Delta T}$ plotted as a function of sample age, t_w ; here, the angle brackets do not indicate a time average, but only a particle average, unlike the MSD. As t_w increases, $\langle \Delta x^2 \rangle$ generally decreases, which is not surprising given the behavior shown in Fig. 1: at large t_w , particle motion on a time scale of $\Delta T = 10$ min reflects the motion of particles confined by their neighbors. However, in addition to this overall relaxation of $\langle \Delta x^2 \rangle$, Fig. 2(a) shows a number of abrupt events, when $\langle \Delta x^2 \rangle$ jumps in value before relaxing further. Further confirmation of the temporally heterogeneous nature of this process is demonstrated by the dashed line in Fig. 2(a), which shows $\gamma = \sqrt{\langle \Delta x^4 \rangle / 3}$. If the dynamics were purely gaussian, i.e. diffusive, we would expect $\gamma = \langle \Delta x^2 \rangle$. The consistently higher value of γ and its prominent correlation to events in $\langle \Delta x^2 \rangle$ indicate that the ensemble dynamics are highly nongaussian and events in $\langle \Delta x^2 \rangle$ particularly so.

It is intriguing that there is no unique behavior for $t_w \approx \Delta T$; instead, aging “events”

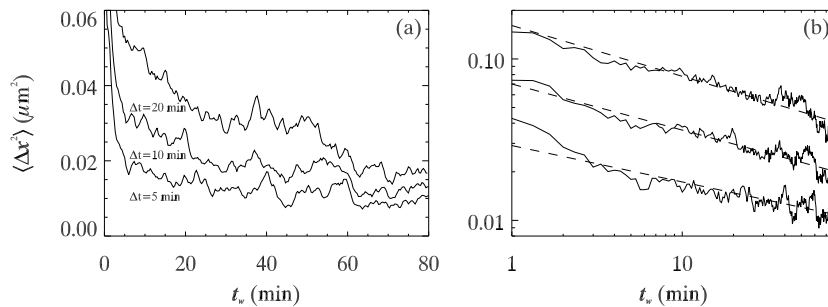


Figure 3. $\langle \Delta x^2 \rangle$ as a function of sample age for various values of lag time, Δt , on linear axes (a) and log-log axes (b). The straight lines in (b) are fits to power law decay, $\langle \Delta r^2 \rangle \sim t_w^{-a}$, with $a=0.23, 0.29,$ and 0.31 for $\Delta t = 5, 10,$ and 20 min, respectively. The curves in (b) corresponding to $\Delta t = 5$ and 20 minutes have been vertically offset for clarity. The data are the same as in the previous figures.

occur at many different values of t_w . To further confirm this, we plot $\langle \Delta x^2 \rangle$ versus sample age for several different values of ΔT in Fig. 3. The curves are clearly related; many events are simultaneously present in all curves. In Fig. 3(b) these curves are plotted on log-log axes, showing that the overall decrease in $\langle \Delta x^2 \rangle$ is consistent with a power law decay, $\langle \Delta x^2 \rangle \sim t_w^{-a}$. For different samples and different choices of ΔT , we find a ranges between 0.05 and 0.5.

In super-cooled colloidal liquids it is known that the dynamics are spatially heterogeneous as well as temporally heterogeneous [7, 8]. To investigate this for our aging samples, we plot the 3D locations of mobile particles in Fig. 4 for $t_w = 10, 55,$ and 95 min. The mobility of a particle is defined as its displacement during the interval t_w to $t_w + \Delta T$ (with $\Delta t = 10$ min). The particles shown are the 10% most mobile at those times, and are generally grouped into large clusters. Varying thresholds does not substantially change these pictures. Our results are similar to the spatial heterogeneities seen in simulations of aging [16]. Signs of heterogeneities have also been seen in aging experiments which studied glycerol [17]. Previous microscopic studies of colloidal glasses did not show such large clusters [7]; we find that the slight averaging of the particle trajectories discussed above (over a 1 min interval) is necessary to distinguish the rearrangements from the local Brownian motion of caged particles. Without averaging, our pictures look similar to those of Ref. [7].

It is striking that the mobile particles are clustered for all values of t_w , notably at both $t_w = 10$ min $= \Delta T$ and $t_w = 95$ min $\gg \Delta T$. We investigate the t_w dependence of the spatial clustering of mobile particles by generating similar pictures for each t_w and measuring the average size of the clusters in each picture. (A cluster is defined as all connected mobile particles which are closer to each other than $3.2 \mu\text{m}$, the first minimum of $g(r)$, the pair correlation function.) Again, mobile particles are defined as the particles with displacements in the top 10% at each t_w , using ΔT to characterize the displacements. The average cluster size shows large fluctuations, as seen in Fig. 2(b). If the 10% most mobile particles were randomly distributed in space, the average cluster

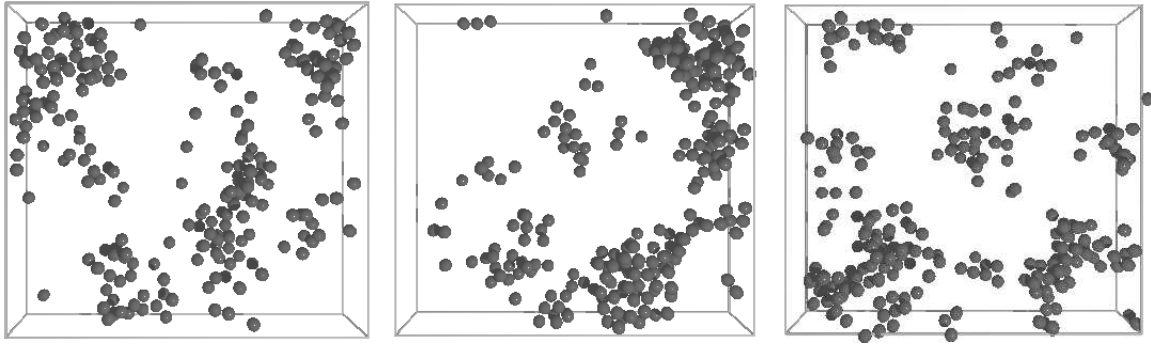


Figure 4. Locations of the 10% most mobile particles at three different ages t_w . For each picture, mobility was determined by calculating displacements Δr over an interval $[t_w, t_w + \Delta T]$, with $\Delta T = 10$ min. Left: $t_w = 10$ min, and $\Delta r > 0.43 \mu\text{m}$ for the most mobile particles. Middle: $t_w = 55$ min, $\Delta r > 0.34 \mu\text{m}$. Right: $t_w = 95$ min, $\Delta r > 0.33 \mu\text{m}$. The data are the same as shown in previous figures, and the choices of t_w correspond to local maxima of γ in Fig. 2(a). The particles are drawn to scale ($2.36 \mu\text{m}$ diameter) and the box shown is the entire viewing volume (within a much larger sample chamber).

size would be ~ 4.5 [dashed line in Fig. 2(b)], however, we find that the average cluster size is always larger than this value. The larger average cluster sizes correspond to locally large values of $\langle \Delta x^2 \rangle$ and γ , seen in Fig. 2(a).

Our most surprising result is that overall, the cluster sizes do not increase dramatically with t_w . For the sample to age, particles must move, and may do so in small groups such as these clusters. For early ages t_w , it might be expected that particle rearrangements may involve very few particles, which can rearrange relatively quickly, thus causing the MSD to have a shorter plateau. For larger t_w , if the rearrangements involved more particles, this would by necessity be more difficult and take longer to occur, thus explaining the slower dynamics reflected in the later MSD curves of Fig. 1. However, this is not what we see. As seen in Fig. 2(b), the average cluster size does not dramatically change as a function of t_w . This remains true even if we scale the choice of Δt with t_w (not shown). Thus, it is not yet clear what ultimately causes the dynamics to slow as our sample ages. While the rearrangements occur via groups such as those shown in Fig. 4, we have not found anything in their character which changes as the sample ages.

While all the data shown in the figures correspond to one sample with $\phi = 0.62$, we have investigated five other samples in the range $0.58 \leq \phi \leq 0.62$. All data sets show similar behavior, and as yet we see no clear ϕ dependence in our results.

4. Conclusions

Aging in our colloidal samples appears to be due to the most mobile particles in the sample, seen in Fig. 4 and reflected by the fluctuations in Fig. 2. In order for the

sample to age, particles must move to new positions. Our results show that such rearrangements are both spatially and temporally heterogeneous. In general, each aging event appears spatially uncorrelated with the previous. The surprising result is that significant fluctuations occur on time scales $\Delta t \ll t_w$, despite the fact that for large t_w , the mean square displacement shows only a plateau at such Δt (see Fig. 1). We find, in fact, that the plateau in the MSD is due to a temporal average over these infrequent rearrangement events and the more prevalent caged behavior. We have also attempted to investigate the behavior of the most immobile particles, but this has been difficult, as every particle still possesses nontrivial Brownian motion, and there is no unambiguous way to distinguish the most immobile particles.

Thus, the changing character of the MSD (Fig. 1) and the related decay in $\langle \Delta x^2 \rangle$ for a fixed Δt (shown in Fig. 3) seem to be the most significant dynamical changes in aging colloidal glasses. In our future work, we plan to investigate the microscopic structural changes associated with these dynamical changes.

5. Acknowledgments

We thank J.-P. Bouchaud and S. Franklin for helpful discussions. This work was supported by NASA and the University Research Committee of Emory University.

References

- [1] Pusey P N and van Megen W 1986 *Nature* **320** 340
Pusey P N and van Megan W 1987 *Phys. Rev. Lett.* **59** 2083
- [2] Bartsch E, Frenz V, Möller S, and Silesco H 1993 *Physica A* **201** 363
- [3] van Megen W and Underwood S M, 1994 *Phys. Rev. E* **49** 4206
- [4] van Blaaderen A and Wiltzius P 1995 *Science* **270** 1177
- [5] Angell C A 2000 *J. Phys. Cond. Mat.* **12** 6463
Ediger M D, Angell C A, and Nagel S R 1996 *J. Phys. Chem.* **100** 13200
- [6] Weeks E R and Weitz D A 2002 *Phys. Rev. Lett.* **89** 095704
- [7] Weeks E R, Crocker J C, Levitt A C, Schofield A, and Weitz D A 2000 *Science* **287** 627
- [8] Kegel W K and van Blaaderen A 2000 *Science* **287** 290
- [9] Bouchaud J P 2000, in *Soft and Fragile Matter: Nonequilibrium Dynamics, Metastability and Flow*, Cates M E and Evans M R, Eds., IOP Publishing (Bristol and Philadelphia) 285-304
- [10] van Megen W, Mortensen T C, Williams S R, and Müller J 1998 *Phys. Rev. E* **58** 6073
- [11] Cipolletti L, Manley S, Ball R C, and Weitz D A 2000 *Phys. Rev. Lett* **84** 2275
- [12] Bonn D, Tanaka H, Wegdam G, Kellay H, Meunier J 1998 *Europhys. Lett.* **45** 52
- [13] Knaebel A, Bellour M, Munch J-P, Viasnoff V, Lequeux F, Harden J L 2000 *Europhys. Lett.* **52** 73
- [14] Dinsmore A D, Weeks E R, Prasad V, Levitt A C, and Weitz D A 2001 *App. Optics* **40**, 4152
- [15] Crocker J C and Grier D G 1996 *J. Colloid Interface Sci.* **179** 298
- [16] Vollmayr-Lee K, Kob W, Binder K, and Zippelius A 2002 *J. Chem. Phys.* **116** 5158
- [17] Miller R S and MacPhail R A 1997 *J. Phys. Chem. B* **101** 8635
- [18] Castillo H B, Chamon C, Cugliandolo L F, Kennett M P 2002 *Phys. Rev. Lett.* **88** 237201